Redundancy Design for Modular Multilevel Converter based STATCOMs

A. F. Cupertino, J. V. M. Farias, H. A. Pereira, S. I. Selem e Jr. and V.N. Ferreira

Published in:

Microelectronics Reliability

DOI (*link to publication from Publisher*):

10.1016%2Fj.microrel.2019.113471

Publication year:

2019

Document Version:

Accepted author manuscript, peer reviewed version

Citation for published version:

A. F. Cupertino, J. V. M. Farias, H. A. Pereira, S. I. S. Junior and V.N. Ferreira, "Redundancy Design for Modular Multilevel Converter based STATCOMs,"Microelectronics Reliability, vol.100-101, September 2019.
doi: 10.1016%2Fj.microrel.2019.113471

Redundancy Design for Modular Multilevel Converter based STATCOMs

João Victor M. Farias[a], Allan F. Cupertino[b,c], Victor de Nazareth Ferreira[c], Heverton A. Pereira[d], Seleme Isaac Seleme Jr.[c]

[a]*Graduate Program in Electrical Engineering, Federal Center for Technological Education of Minas Gerais, Belo Horizonte, MG, Brazil*
[b]*Department of Materials Engineering, Federal Center for Technological Education of Minas Gerais, Belo Horizonte - MG, Brazil*
[c]*Graduate Program in Electrical Engineering, Federal University of Minas Gerais, Belo Horizonte - MG Brazil*
[d]*Department of Electrical Engineering, Federal University of Viçosa, Viçosa, MG, Brazil*

Abstract

Many strategies have been proposed to improve the reliability of Modular Multilevel Converters (MMCs). However, the redundancy factor selection to support a converter fault tolerance operation is an important field to be explored. This work proposes a combined reliability model for the correct selection of the additional number of cells to achieve a target lifetime. This model combines both wear-out and random failures data and compute the required redundancy factor for a given reliability target. The proposed model is evaluated through a reliability-oriented case study, whereas four device voltage classes in a 13.8 kV/17 MVA MMC STATCOM are considered.

Keywords: Modular Multilevel Converters, Reliability, Redundancy Design, Wear-out Failures, Random Failures .

1. Introduction

Modular multilevel converter (MMC) is considered the next generation of converter for medium and high voltage applications [1]. Among the MMC topologies, the single-delta bridge cell (SDBC) is generally used in STATCOM and energy storage applications. Moreover, the double-star chopper cells (DSCC) is widely employed in STATCOM, HVDC and in some applications from electrical drives systems [2, 3]. The MMC topologies consist of the cascaded connection of low voltage bridges, aiming to achieve a high voltage capability. Nevertheless, in some applications, it is necessary to associate a large number of cells, compromising the system-level reliability. Therefore, the MMCs reliability has been receiving a huge attention in the last years.

Some works propose a Design for Reliability (DfR) approach as a solution to ensure a target lifetime for the power converters [4]. In this concept, the design is accomplished to avoid the system to move forward to the wear-out zone, where the failure rate grows faster, as shown in Fig. 1 [5]. As a result, the probability of wear-out failures can be reduced during the design phase. Although the wear-out failures can be predicted and even avoided, the catastrophic events are unpredictable and are defined by constant failure rate [6]. Thereby, to overcome these events, redundant cells shall be added during the converter design.

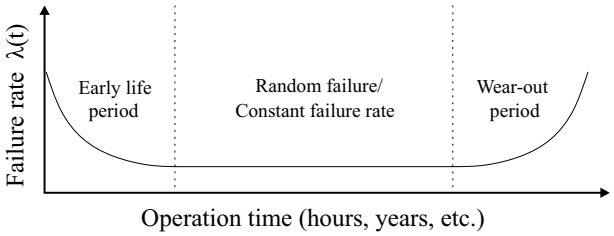

Figure 1: Typical failure rate curve — bathtub curve.

The redundancy factor can be defined as the number of additional cells to ensure the converter operation after a predefined number of failures [7]. An empirical redundancy factor of 10% is proposed in [1]. On the other hand, some works propose the evaluation of the redundancy factor based on the failure rate of the devices [8, 9, 10]. Nevertheless, these works only consider the constant failure rate region of the bathtub curve, shown in Fig. 1. Hence, the only reliability tool considered in these models is the FIT (failure in time),

Email addresses: joaofariasgv.jvmf@gmail.com (João Victor M. Farias), afcupertino@ieee.org (Allan F. Cupertino), vnferreira89@gmail.com (Victor de Nazareth Ferreira), heverton.pereira@ufv.br (Heverton A. Pereira), seleme@cpdee.ufmg.br (Seleme Isaac Seleme Jr.)

which is defined by the number of random failures during a specific time.

Although reliability-based strategies have been proposed for MMCs [8, 9, 10], the redundancy factor selection considering both influence of constant and wear-out regions still missing. Therefore, this work proposes a combined reliability model to select the correct redundancy factor, to achieve a target lifetime, even with a predefined number of random failures. To evaluate this concept, a reliability-based case study is conducted considering different redundancy factors for four device voltage classes in a 13.8 kV/17 MVA MMC STATCOM.

This paper is outlined as follows. The design of the MMC-STATCOM is described in Section 2. Section 3 presents the combined reliability modeling. In section 4 this model is evaluated through a reliability-based case study. Section 5 presents the results obtained. Finally, the conclusions of this work are stated in Section 6.

2. The DSCC-MMC STATCOM

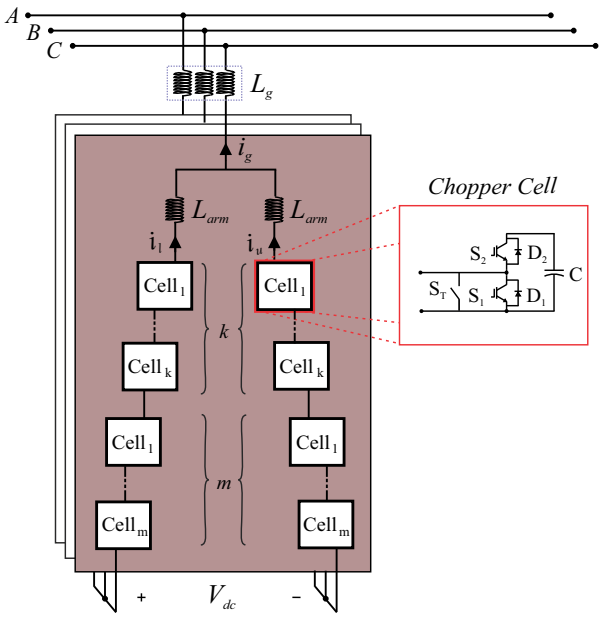

Figure 2: Schematic of the DSCC-MMC STATCOM.

The three-phase MMC in double-star configuration is presented in Fig 2. The impedance L_g represents the converter connection to the grid. The six MMC arms are composed by an inductor L_{arm}, k non-redundant cells and m redundant cells per arm. The total number of cells per arm is n, where $n = k + m$. All cells consist of two IGBTs S_1 and S_2, two antiparallel connected diodes D_1 and D_2, an energy storage capacitor C. There is usually a switch S_T in parallel with the cell, bypassing it in case of failures.

3. Reliability Modeling

The reliability function $R(t)$ and failure rate $\lambda(t)$ are highly important tools for reliability modeling. $R(t)$ represents a group of samples that can properly work during a specific time, and the $\lambda(t)$ is the failure rate of a system. As shown in Fig. 1, $\lambda(t)$ varies regarding the specific operation region. The early period is defined by manufacturing constraints and it is infeasible to deal with it in the application level. Nevertheless, the constant failure region and wear-out period depend on failure events and system behavior. Thereby, reliability-based strategies can be applied to control the failure rate and ensure continuity of service during a target lifetime. In this section, the reliability modeling of a MMC in both failure regions is described.

3.1. Constant Failure Region

In the constant failure region, the same failure rate for the devices is considered. Hence, the cell-level reliability function is given by [9]:

$$R_{cell,cf}(t) = e^{-\lambda_{cell}t}, \tag{1}$$

where λ_{cell} its failure rate. Assuming that the failure rate of each IGBT module is independent, the cell-level failure rate is $\lambda_{cell} = 2\lambda_{IGBT}$. The failure rate depends on the technological complexity of the devices and some factors that can be included in the λ_{IGBT} formulation as given by:

$$\lambda_{IGBT} = \lambda_b \pi_T \pi_S \pi_A, \tag{2}$$

where λ_b is the component base failure rate, π_T is the temperature factor, π_S is the electric stress factor, π_A is the application factor. For standard power modules (IGBT with anti-parallel diode), a base failure rate of 100 FIT is commonly employed [9]. The factors are given by:

$$\pi_T = e^{-2114\left(\frac{1}{T_j+273}-\frac{1}{298}\right)}, \tag{3}$$

$$\pi_S = 0.045e^{3.1V_s}, \tag{4}$$

$$\pi_A = \begin{cases} 0.7 & switching \\ 1.5 & linear\ application \end{cases} \tag{5}$$

where V_s is the voltage stress factor and T_j is the device junction temperature.

3.2. Wear-out Failure Region

The failure rate evolution in the wear-out region can be modeled as illustrated in Fig. 3. Initially, the mission profiles are defined. The conduction, switching losses and thermal impedances of the power modules are obtained from look-up tables based on the datasheets. The hybrid thermal model proposed by [11] is employed in order to estimate the junction (T_j) and case temperature (T_c) of each power device.

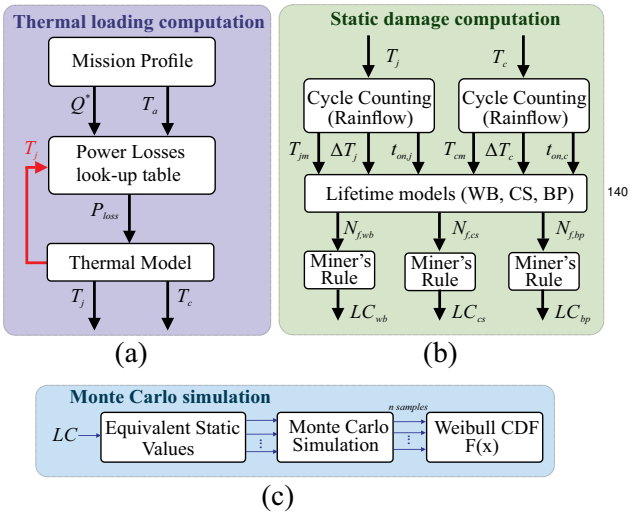

Figure 3: Wear-out analysis flowchart: (a) Translation of the mission profile into thermal stresses; (b) Static damage computation through reliability model; (c) Monte Carlo simulation for computation of component and system-level reliability.

The static damage is calculated from the lifetime model provided by ABB for HiPak IGBT power modules [12]. Based on the converter profile, a rainflow counting method is employed [13] in order to identify the characteristics of each cycle. The lifetime model returns the number of cycles to failure N_f of the bond wire (BW), chip solder (CS) and baseplate solder (BP) using the 10% failure rate approach (B_{10} lifetime). Thus, the life consumption (LC) of the devices is obtained from Palmgren-Miner's rule [14].

Since the power devices presents parametric variations due to the manufacturing process and stress variation [15], the lifetime is usually expressed in terms of probabilities. Therefore, the dynamic values obtained by rainflow algorithm are transformed into equivalent static values. Then, a statistical analysis based on Monte-Carlo simulation is performed [16]. The lifetime distribution obtained from Monte Carlo simulation is fitted with the Weibull PDF $f(x)$ [15], where x is the operating time. The cumulative density function (CDF), also called unreliability function $F(x)$, is obtained through the integral of PDF. Since only the reliability of the power devices is taken into account in this study (i.e., S_1, S_2, D_1 and D_2), the unreliability function for each MMC chopper cell can be calculated as:

$$R_{cell,wf}(x) = \prod_{i=1}^{4} (1 - F_{Comp(i)}(x)), \tag{6}$$

where $F_{Comp(i)}(x)$ is the unreliability function of each power device.

3.3. System-level reliability

Assuming that each cell is independent and identical, the complete cell-level reliability can be realized through the product of constant and wear-out reliability functions [5], as follows:

$$R_{cell}(x) = R_{cell,cf}(x) R_{cell,wf}(x). \tag{7}$$

Therefore, the MMC arm-level reliability function can be evaluated as follows [17]:

$$R_{arm}(x) = \prod_{l=1}^{k} R_{cell(l)}(x). \tag{8}$$

However, Eq. (8) is suitable only when non-redundant cells are employed. Basically, the redundant cells are usually operated in active mode or standby mode. The active mode operates with or without load-sharing effect [18]. In this work, only active redundant cells operating without load-sharing effect are taken into account. Thus, when one component fails, the load on the remaining surviving functional components is not changed. Therefore, the MMC arm-level reliability can be evaluated through the *k-out-of-n* model, given by [9]:

$$R'_{arm}(x) = \sum_{p=k}^{n} C_n^p R_{cell}(x)^p (1 - R_{cell}(x))^{n-p}. \tag{9}$$

In general, Eq. (9) is reduced to the Eq. (8) for $n = k$. Thus, the MMC system-level reliability is given by:

$$R_{MMC}(x) = \prod_{l=1}^{6} R'_{arm}(x). \tag{10}$$

4. Redundancy Factor Design

From the industry point of view, the converter shall be designed to achieve a reliability level $R(x_0)$ for a defined target lifetime x_0, regarding its specific application [19]. Therefore, this work proposes a scheme to evaluate a redundancy factor to satisfy a pre-defined criterion of MMC reliability. Thus, a combined reliability model that includes both constant and wear-out regions is used, as described in Eq. (10). The redundancy factor design flowchart is shown in Fig 4.

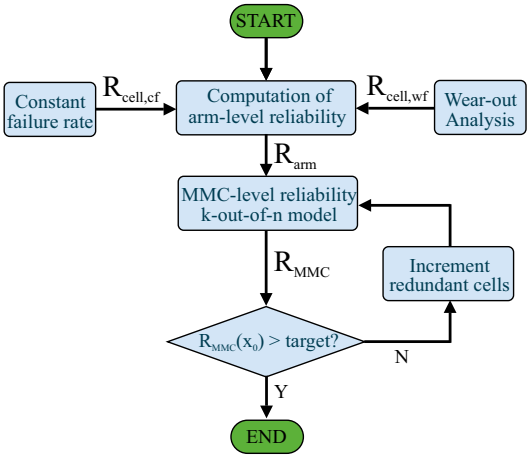

Figure 4: Flowchart for the redundancy factor design.

Initially, the cell reliability is calculated by Eq. (7). Thus, the MMC system-level reliability can be evaluated by Eq (10). Afterward, the MMC reliability is analyzed for a given lifetime target. Since the required MMC reliability is not met (i.e., Eq. (10) $< R(x_0)$), redundant cells shall be employed. Then, the number redundant cells (m) is incremented until the reliability criterion is reached (i.e., Eq. (10) $> R(x_0)$). Finally, the minimum required redundancy factor can be obtained as follows:

$$RF = \frac{m}{k}, \tag{11}$$

5. Case Study

Based on the topology presented in Fig. 2, the simulations were performed using the PLECS and MATLAB software systems, aiming to estimate the lifetime, energy losses and cost of each design. A 17 MVA MMC-STATCOM with line voltage of 13.8 kV at the point of common coupling (PCC) is considered. The control strategy used in this work is based on reference [20]. Table 1 presents the main circuit parameters. The converter is submitted to a mission profile based on a reactive power (Q) and ambient temperature (T_a) measurements in southeastern Brazil, as presented in Fig. 5.

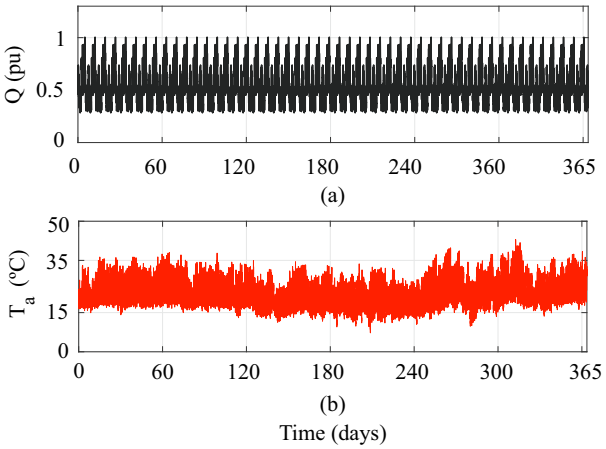

Figure 5: Mission profiles with a sampling time of 5 min: (a) Reactive Power; (b) Ambient Temperature.

Table 1: Main parameters of the MMC for four proposed designs.

Parameters		MMC specifications			
		C_1	C_2	C_3	C_4
k		33	17	13	9
V_{dc}	(kV)	28	28	28	28
V_{svc}	(kV)	1.7	3.3	4.5	6.5
V^*_{cell}	(kV)	0.85	1.65	2.15	3.11
$I_{arm,rms}$	(A)	460	460	460	460
C_{cell}	(mF)	9.54	4.92	3.76	2.61
L_{arm}	(mH)	4.46	8.70	11.82	17.08
L_g	(mH)	1.5	1.5	1.5	1.5
f_{sw}	(Hz)	210	210	210	210
R_{ha}	(K/W)	0.13	0.07	0.05	0.03

Table 2 shows the part numbers employed in the MMC designs. Four different ABB HiPak IGBTs modules solutions with blocking voltage capability range between 1.7 kV and 6.5 kV are considered. Commercially available modules with rated current close to 800 A are selected. The heatsinks are evaluated in order to ensure similar temperature stresses (i.e., T_j below 150 °C) in each IGBTs module solution [20].

The typical lifetime target of power electronics systems, from industry perspective, is described in [21]. For STATCOM applications, such as industrial and wind power systems, it is reported an expected lifetime of around 20 years [21, 19]. Thereby, the MMC lifetime

Table 2: HiPak IGBT modules specifications for four proposed solutions.

Voltage (V)	Current (A)	Part Number	Case
1700	800	5SND 0800M170100	C_1
3300	800	5SNA 0800N330100	C_2
4500	800	5SNA 0800J450300	C_3
6500	750	5SNA 0750G650300	C_4

target is defined as $x_0 = 20$ years of operation. From the B_1 lifetime approach, the MMC reliability $R(x_0 = 20) > 0.99$ is applied.

The overall cost of each design is mainly related to investment in power electronics [22] and the semiconductor conduction and switching losses [9]. Therefore, the overall cost is given by:

$$Cost = nK_c V_{svc} I_{svc} + K_o E_c, \quad (12)$$

where V_{svc} is the device voltage class and I_{svc} is the rated device current. $K_c = 3.5$ €/kVA is employed [22] in this work. Based on loss penalty for transmission system, the price per kilowatt-hour is $K_o = 0.11$ €/kWh [23]. Moreover, E_c is the converter energy consumption. Thus, $E_{c_{20}}$ is defined as the converter energy consumption for $x_0 = 20$ years.

6. Results

Fig. 6 presents the junction temperature in D_2 for all solutions. Based on the mission profile application, the diode D_2 is the most stressed device in a cell. As observed, the maximum junction temperature is approximately 120 °C. All cases have similar thermal stresses.

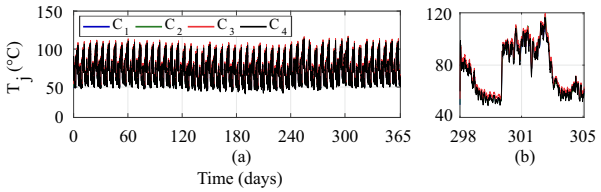

Figure 6: (a) Junction temperatures of the more stressed device D_2 in a cell for 4 designs; (b) Detailed view of (a).

Considering the $T_{jmax} = 120$ °C, the IGBT failure rate is calculated by Eq. 2, as shown in Table 3. C_1 presents the lowest FIT among the solutions.

Since the thermal cycling is obtained, the rainflow algorithm and the lifetime model are applied. Table 4 presents the static LC in one year for the critical joints of the power devices based on C_1 solution. The

Table 3: Parameters for evaluation of IGBT failure rate for different MMC design.

Parameters	C_1	C_2	C_3	C_4
π_T	5.12	5.53	5.59	5.39
π_S	0.21	0.21	0.20	0.20
π_A	0.70	0.70	0.70	0.70
λ_{IGBT} (FIT)	75.26	81.29	78.26	75.46

Table 4: Static LC of devices by different joints based on C_1 solution.

Devices	BW	CS	BP
S_1	$4.24 \cdot 10^{-13}$	$2.29 \cdot 10^{-6}$	$1.28 \cdot 10^{-3}$
S_2	$4.49 \cdot 10^{-13}$	$2.30 \cdot 10^{-6}$	$1.30 \cdot 10^{-3}$
D_1	$7.38 \cdot 10^{-13}$	$2.46 \cdot 10^{-6}$	$1.56 \cdot 10^{-3}$
D_2	$9.37 \cdot 10^{-13}$	$2.49 \cdot 10^{-6}$	$1.58 \cdot 10^{-3}$

baseplate solder is the most damaging factor. Therefore, in the Monte-Carlo simulation, the wear-out failure in the baseplate solder is analyzed [16].

Fig. 7 presents both wear-out and constant failure rates contributions on the MMC system-level reliability. The contribution of each failure rate in the system reliability is derived from Eq. (7). For the sake of simplicity, only the solution C_1 is illustrated in Fig. 7. As observed, the most significant contribution in the MMC reliability is given by the constant failure rate in the initial years. In addition, the wear-out failure influences the reliability of the converter close to converter end-of-life.

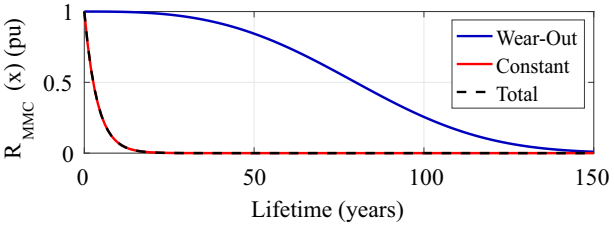

Figure 7: MMC system-level reliability based on C_1: wear-out and constant failure rates contributions factors and the total converter reliability.

The MMC system-level reliability for the four analyzed cases are shown in Fig. 8. As observed, solutions with the highest number of cells present smaller system-level reliability. The solution based on the design C_4 presents the highest reliability, 25.96%. Furthermore, C_1 has the lowest reliability, 0.67%. All solutions present reliability below the defined target. Therefore, the redundancy factor design should be applied.

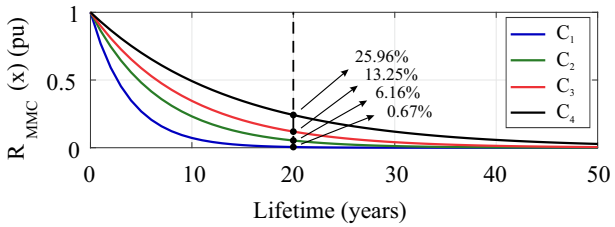

Figure 8: MMC system-level reliability function for different solutions.

The redundancy factor effect in solution C_1 is analyzed in Fig. 9. As observed, when $m > 4$, the target is reached: $R(20) > 0.99$. For $m > 6$, the increase in the number of redundant cells does not considerably affect the MMC system-level reliability. Fig. 10 presents the variation of the MMC system-level reliability as function of the redundancy factor for design C_1. As observed, $R(20) = 0.67\%$ for $m = 0$. The system-level reliability is increased to 99.79% when a $RF = 15.15\%$ is applied, which corresponds to $m = 5$.

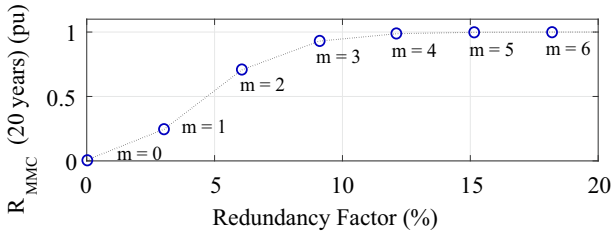

Figure 9: MMC system-level reliability in 20 years based on C_1 with different redundancy factors.

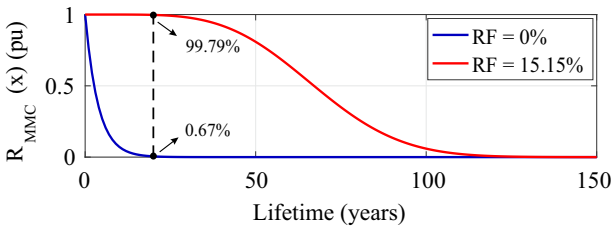

Figure 10: MMC system-level reliability function based on C_1 for 2 different redundancy factors.

Table 5 summarizes the results for all solutions proposed in this work. The index 20 indicates that the parameter was applied to the required target. $E'_{c_{20}}$ and $Cost'$ are the parameters based on the required redundancy factor RF' for each design. As observed, when voltage rating of the power devices increases, the required redundancy factor increases. This is related to the number of converter cells (which reduces when the voltage increases) and with rounding (since the number of redundant cells must be integer). Although C_2 presents the lowest energy consumption, the best cost-benefit for the B_1 approach refers to C_1.

Table 5: Comparison of the redundant proposed designs for B_1 lifetime approach ($R(20) = 99\%$).

Parameters	**C$_1$**	**C$_2$**	**C$_3$**	**C$_4$**
RF' (%)	15.15	17.65	23.08	33.33
E'c_{20} (GWh)	10.06	9.69	10.32	10.63
Cost' (M€)	3.49	3.52	3.87	4.08

Finally, Fig. 11 presents the solutions cost for different reliability levels. As expected, the higher the system-level reliability required, the greater the cost of the solution. As can be seen, a line is traced for the best trade-off between cost and system-level reliability. The C_1 solution with $m = 3$ ($RF = 9.09\%$) is the most suitable design for a reliability level greater than 90%. However, for more conservative designs, a reliability level $R(20) = 99\%$ can be achieved with class C_1 and five redundant cells ($RF = 15.15\%$). In this case, the cost is increased by 5.56 % for this extra reliability level.

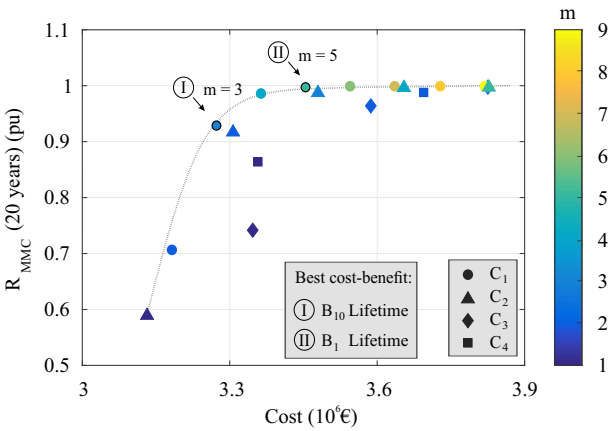

Figure 11: *Reliability x cost* of all MMC solutions for different redundancy factors, considering a lifetime target of 20 years.

7. Conclusions

This work proposed a combined reliability model for correct selection of the number of redundancy cells to achieve a target lifetime. Both random and wear-out failures are considered in the model. As observed, random cells failures are dominant in the converter. Nevertheless, wear-out failure has an influence on the converter reliability close to the end-of-life period.

Four different realizations of the MMC-STATCOM were compared in terms of cost and power losses. As a result, 1.7 kV is the most cost-effective solution to achieve 99% of reliability level, during the whole target lifetime. It was concluded that the redundancy factor shall be chosen to achieve the required reliability with the minimum number of redundant cells.

The proposed methodology can be easily extended to other converter topologies and adapted for different cost evaluation methodologies. Finally, the most cost-effective solution for different reliability criteria can be evaluated.

8. Acknowledgement

The authors would like to thank the Brazilian agencies CNPq, CAPES and FAPEMIG by funding.

References

[1] N. Ahmed, L. Ängquist, A. Antonopoulos, L. Harnefors, S. Norrga, H. Nee, Performance of the modular multilevel converter with redundant submodules, in: IECON, 2015, pp. 003922–003927.

[2] H. Akagi, Multilevel converters: Fundamental circuits and systems, Proc. IEEE 105 (11) (2017) 2048–2065.

[3] H. Akagi, Classification, terminology, and application of the modular multilevel cascade converter (mmcc), in: The 2010 International Power Electronics Conference - ECCE ASIA -, 2010, pp. 508–515. doi:10.1109/IPEC.2010.5543243.

[4] F. Blaabjerg, D. Zhou, A. Sangwongwanich, H. Wang, Design for reliability in renewable energy systems, in: Int. Symp. Power Electron., 2017, pp. 1–6.

[5] U. Scheuermann, M. Junghaenel, Limitation of power module lifetime derived from active power cycling tests, in: CIPS 2018.

[6] F. Iannuzzo, Short-circuit robustness assessment in power electronic modules for megawatt applications, Facta universitatis-series: Electron. and Energetics (2016) 35–47.

[7] J. Xu, P. Zhao, C. Zhao, Reliability analysis and redundancy configuration of mmc with hybrid submodule topologies, IEEE Trans. Power Electron. 31 (4) (2016) 2720–2729.

[8] J. Xu, H. Jing, C. Zhao, Reliability modeling of mmcs considering correlations of the requisite and redundant submodules, IEEE Trans. Power Del. 33 (3) (2018) 1213–1222.

[9] P. Tu, S. Yang, P. Wang, Reliability- and cost-based redundancy design for modular multilevel converter, IEEE Trans. Ind. Electron. 66 (3) (2019) 2333–2342.

[10] M. Alharbi, S. Isik, S. Bhattacharya, Reliability comparison and evaluation of mmc based hvdc systems, in: IEEE eGrid, 2018.

[11] K. Ma, N. He, M. Liserre, F. Blaabjerg, Frequency-domain thermal modeling and characterization of power semiconductor devices, IEEE Trans. Power Electron. 31 (10) (2016) 7183–7193.

[12] ABB, Load-cycling capability of hipak igbt modules, Application note.

[13] H. Liu, K. Ma, Z. Qin, P. C. Loh, F. Blaabjerg, Lifetime estimation of mmc for offshore wind power hvdc application, IEEE JESTPE 4 (2) (2016) 504–511.

[14] H. Huang, P. A. Mawby, A lifetime estimation technique for voltage source inverters, IEEE Trans. Power Electron. 28 (8) (2013) 4113–4119.

[15] A. Sangwongwanich, Y. Yang, D. Sera, F. Blaabjerg, Lifetime evaluation of grid-connected pv inverters considering panel degradation rates and installation sites, IEEE Trans. Power Electron. 33 (2) (2018) 1225–1236.

[16] R. de Sousa, J. Farias, A. Cupertino, H. Pereira, Life consumption of a mmc-statcom supporting wind power plants: Impact of the modulation strategies, Microelectron. Reliab. 88-90 (2018) 1063 – 1070, esref 2018.

[17] B. Wang, X. Wang, Z. Bie, P. D. Judge, X. Wang, T. C. Green, Reliability model of mmc considering periodic preventive maintenance, IEEE Trans. Power Del. 32 (3) (2017) 1535–1544.

[18] Y. Chen, X. Yu, Y. Li, A failure mechanism cumulative model for reliability evaluation of a k-out-of-n system with load sharing effect, IEEE Access 7 (2019) 2210–2222. doi:10.1109/ACCESS.2018.2852730.

[19] H. Wang, M. Liserre, F. Blaabjerg, P. de Place Rimmen, J. B. Jacobsen, T. Kvisgaard, J. Landkildehus, Transitioning to physics-of-failure as a reliability driver in power electronics, IEEE JESTPE 2 (1) (2014) 97–114.

[20] J. V. M. Farias, A. F. Cupertino, H. A. Pereira, S. I. S. Junior, R. Teodorescu, On the redundancy strategies of modular multilevel converters, IEEE Trans. Power Del. 33 (2) (2018) 851–860.

[21] J. Falck, C. Felgemacher, A. Rojko, M. Liserre, P. Zacharias, Reliability of power electronic systems: An industry perspective, IEEE Industrial Electronics Magazine 12 (2) (2018) 24–35. doi:10.1109/MIE.2018.2825481.

[22] H. A. B. Siddique, A. R. Lakshminarasimhan, C. I. Odeh, R. W. D. Doncker, Comparison of modular multilevel and neutral-point-clamped converters for medium-voltage grid-connected applications, in: ICRERA, 2016, pp. 297–304.

[23] R. Alvarez, M. Wahle, H. Gambach, J. Dorn, Optimum semiconductor voltage level for mmc submodules in hvdc applications, in: EPE'16 ECCE Europe, 2016, pp. 1–9.